Published in final edited form as:
Fertil Steril. 2013 February ; 99(2): 558–564. doi:10.1016/j.fertnstert.2012.10.027.

QUANTIFICATION OF NUCLEOLAR CHANNEL SYSTEMS: UNIFORM PRESENCE THROUGHOUT THE UPPER ENDOMETRIAL CAVITY

Michael J. Szmyga, M.S.[1], **Eli A. Rybak, M.D., M.P.H.**[1,2,5], **Edward J. Nejat, M.D., M.B.A.**[1,2], **Erika H. Banks, M.D.**[2], **Kathleen D. Whitney, M.D.**[3], **Alex J. Polotsky, M.D., M.S.**[2,6], **Debra S. Heller, M.D.**[4], and **U. Thomas Meier, Ph.D.**[1,8]

[1] Department of Anatomy and Structural Biology, Albert Einstein College of Medicine, Bronx, NY

[2] Department of Obstetrics & Gynecology and Women's Health, and Albert Einstein College of Medicine, Bronx, NY

[3] Department of Pathology, Albert Einstein College of Medicine, Bronx, NY

[4] Department of Pathology, UMDNJ – New Jersey Medical School, Newark, NJ

Abstract

Objective—To determine the prevalence of nucleolar channel systems (NCSs) by uterine region applying continuous quantification.

Design—Prospective clinical study.

Setting—Tertiary care academic medical center.

Patients—42 naturally cycling women who underwent hysterectomy for benign indications.

Intervention—NCS presence was quantified by a novel method in six uterine regions, fundus, left cornu, right cornu, anterior body, posterior body, and lower uterine segment (LUS), using indirect immunofluorescence.

Main Outcome Measures—Percent of endometrial epithelial cells (EECs) with NCSs per uterine region.

Results—NCS quantification was observer-independent (intraclass correlation coefficient [ICC] = 0.96) and its intra-sample variability low (coefficient of variability [CV] = 0.06). 11/42 hysterectomy specimens were midluteal, 10 of which were analyzable with 9 containing over 5% EECs with NCSs in at least one region. The percent of EECs with NCSs varied significantly

[8]**Corresponding Author:** U. Thomas Meier, Ph.D. Department of Anatomy and Structural Biology Albert Einstein College of Medicine 1300 Morris Park Avenue Bronx, NY 10461 tom.meier@einstein.yu.edu Phone: 718-430-3294 Fax: 718-430-8996.
[5]Present Address: Reproductive Medicine Associates of New Jersey, Morristown, NJ, USA
[6]Present Address: Department of Obstetrics & Gynecology, University of Colorado, Denver, CO, USA

Conflict of Interest (for all authors): NONE

Authors' Roles
E.A.R., M.J.S., E.J.N., E.H.B. and K.D.W. executed the study; M.J.S., E.A.R., and E.J.N. carried out NCS quantification; D.S.H. performed histologic dating; E.A.R, M.J.S., A.J.P., E.J.N. and U.T.M. analyzed the data; E.A.R. and U.T.M. designed the study and wrote the manuscript.

between the lower uterine segment (6.1%; IQR = 3.0-9.9) and the upper five regions (16.9%; IQR = 12.7-23.4) with fewer NCSs in the basal layer of the endometrium (17% +/−6%) versus the middle (46% +/−9%) and luminal layers (38% +/−9%) of all six regions).

Conclusions—NCS quantification during the midluteal phase demonstrates uniform presence throughout the endometrial cavity, excluding the LUS, with a preference for the functional, luminal layers. Our quantitative NCS evaluation provides a benchmark for future studies and further supports NCS presence as a potential marker for the window of implantation.

Keywords

nucleolar channel system (NCS); endometrium; receptivity; secretory transformation

INTRODUCTION

The nucleolar channel system (NCS) is an enigmatic structure associated with secretory transformation of the endometrium (1). Discovered on the ultrastructural level a half-century ago (2), the NCS is a membranous organelle of uniform size, ~1 μm diameter, that develops transiently in the nuclei of secretory-phase endometrial epithelial cells (EECs; 3-5). In prior work, we established a light microscopic method to stain and identify NCSs via an immunofluorescence approach using an antibody directed against a subset of nuclear pore complex proteins, major components of the NCS (6). We determined that NCSs are present in roughly half of all EEC nuclei during a period overlapping with the implantation window: cycle days (CD) 19-24 of an idealized 28-day cycle. The NCS is specific to healthy, human EECs: It is not detected in endometrial stromal cell nuclei, human breast or gastrointestinal tract tissue, endometrial carcinoma specimens, or in baboon endometrium (6). Moreover, midluteal NCS presence is robust and independent of fertility status including unexplained infertility (7-9).

Given this robust midluteal appearance of NCSs, their sensitivity to progesterone, and absence in pregnancy, among other evidence, we submit that they play a role in endometrial receptivity (5,10-15). Although the literature is sparse regarding possible regional disparities in endometrial receptivity, it is interesting to note that ultrastructural evidence indicates localized concentrations of NCSs (16). The preferred location within the endometrial cavity for blastocyst implantation in both spontaneous and assisted conception, however, is neither clearly known nor well studied. Table 1 lists several reports that have investigated the endometrial region-specific implantation frequency of blastocysts via anatomic dissection or ultrasonography (17-20). These studies collectively suggest that the cornual region might prove most favorable for blastocyst implantation. Accordingly, we hypothesized that NCS presence varies by uterine region and sought to determine the regional prevalence of NCSs within the endometrial cavity. To fully appreciate NCS prevalence and to provide a benchmark for future studies, we developed an absolute NCS quantification method based on our semi-quantitative light microscopic detection method (6).

MATERIALS AND METHODS

Specimens

Uterine specimens were obtained from patients who underwent hysterectomy for benign gynecologic indications (predominantly menorrhagia attributed to uterine fibroids) at Montefiore Medical Center, Weiler Division, a tertiary-care academic medical center in the Bronx, NY affiliated with the Albert Einstein College of Medicine, from November 2008 through August 2009. Institutional review board (IRB) approval was obtained for this study. Specific patient data were de-identified. Clinical information provided for each specimen was limited to a de-identified final pathology report and to data transcribed by the operating team on a “study sheet” that was distributed by the operating room nursing staff prior to every hysterectomy case, and which accompanied the specimen from the operating room to the surgical pathology department. Enrollment criteria were established in an effort to enroll all women who were postovulatory (based on a self-reported LMP). Exclusion criteria fell under three categories: First, any case with known or suspected malignancy or endometrial hyperplasia was excluded. Logistically, such cases warranted more extensive endometrial sampling and longer-term preservation of the hysterectomy specimens for clinical purposes. Moreover, NCS presence has not been detected in cases of endometrial adenocarcinoma (6). Second, any case involving morcellation of the uterus (i.e. laparoscopic supracervical hysterectomy) was excluded given the obvious inability to identify specific uterine regions. Finally, any specimen deemed unlikely to demonstrate secretory-phase endometrium was excluded at the outset. Specifically, if the patient's self-reported LMP, as recorded in the preoperative nurse interview, was less than ten days prior to surgery, or if the patient was exposed to gonadotropin releasing hormone agonist (i.e. leuprolide) or to any estrogen and/or progestin therapy during the 3-month preoperative period, or if the patient was aged 50 or older, then the appropriate check boxes on the study sheet would trigger exclusion of the specimen from the study.

Background information

The following information was obtained by the surgical team after reviewing the preoperative history form in the patient's chart, and then entered onto the study sheet: patient's age, parity, self-reported LMP, past obstetric and gynecologic surgical history, and indication for hysterectomy. Additionally, the type of hysterectomy performed (abdominal versus vaginal versus laparoscopic; total versus supracervical) was recorded. In addition to diagnosing and describing any pathology, the final pathology report detailed the uterine weight and the presence and location (intramural versus submucosal versus subserosal) of any fibroids. Of note, the pathologist labeled each endometrium as secretory, proliferative, or inactive. Slides from uteri determined to be secretory were subsequently provided to another pathologist (DSH) with specific expertise in classical histologic dating using Noyes criteria (21) given the obvious limitations with relying solely on the self-reported LMP. Recognizing, however, the substantial intersubject, intrasubject, and interobserver variability that limit the precision of histologic dating using Noyes criteria (22), we limited our use of histologic dating to merely identify the specimens that demonstrated a histologic date between cycle day (CD) 18-24, inclusively, and were thereby deemed to be midluteal.

Processing and immunostaining of tissue sections

Upon removal from the pelvis, uterine specimens were transported immediately for sectioning by the surgical pathology staff. If the uteri could not be sectioned within 15 minutes, before placing them in 10% formalin, they were sliced coronally through the endometrium to minimize endometrial autolysis that could adversely affect subsequent immunostaining (23,24). Sections of endometrium were obtained from six different regions of the endometrial cavity: fundus, left cornu, right cornu, anterior body, posterior body, and LUS. The tissue samples were then paraffin embedded, sectioned, and mounted on slides.

Immunostaining was performed as previously described (6,7). Briefly, tissue sections were deparaffinized, rehydrated, and (for antigen retrieval) treated with 10mM sodium citrate (pH 6.0). The slides were then immersed in −20°C methanol for 5 minutes in order to optimize immunostaining. After complete air-drying, the slides were rehydrated with phosphate-buffered saline (PBS). NCSs were detected by indirect immunofluorescence using the monoclonal antibody 414 (mAb414; Covance, Princeton, NJ) and DyLight488 labeled secondary antibodies (Jackson ImmunoResearch, West Grove, PA), as previously described (6). Nuclei were detected by staining with 4’,6-diamidino-2-phenylindole (DAPI) at 1μg/ml. For preservation, samples were post-fixed with 4% paraformaldehyde. All tissue samples were analyzed for the presence of NCSs by two independent observers as described previously (7) and the samples from the uteri with over 5% EECs with NCSs in at least one region were fully quantified by the newly developed method described below.

Imaging and quantification of NCSs

All samples were imaged on a DeltaVision Core system (Applied Precision, Issaquah, WA) with an Olympus IX71 stand using a 60X/1.42 NA planapo objective and a Photometrics (Tucson, AZ) CoolSnap HQ2 CCD camera. To be blinded regarding NCS presence, 10 areas/fields with endometrial glands of each paraffin section were randomly selected based on nuclear DNA staining using the DAPI channel. Subsequently, Z-series of optical planes across the entire paraffin section were collected in 0.3 μm steps in both, DAPI (to count nuclei/EECs) and FITC (to count NCSs) channels. For deconvolution, softWoRx 3.6.0 (Applied Precision, Issaquah, WA) was used with the enhanced ratio method, medium filter, and 10 iterations. Deconvolved Z-series were viewed in ImageJ (National Institutes of Health, Bethesda, MD). Staining of nuclear pore complexes by mAb414 served as internal control for the staining procedure and sections were only analyzed if the pores could be clearly distinguished (Fig. 1A). NCSs and EEC nuclei were analyzed manually using the ImageJ multi-point tool to mark and count each NCS and nucleus. Nuclei were counted in a maximum projection of all planes of one area/field. NCSs were counted in each individual plane, viewed as image series to verify in adjacent planes that the signal was gradually lost thereby identifying the structures as the 1 μm-diameter NCSs not only within the plane but in all dimensions (Fig. 1A). The number of NCSs in 10 random areas/fields was summed and divided by the number of EEC nuclei to obtain the % EECs with NCSs for each specimen. In this manner, between 459 and 1182 EECs (765 +/−154) were counted for each of the 53 samples (one section had insufficient epithelial tissue for analysis). A total of 40,565 nuclei and 7,471 NCSs were counted.

The method was validated on a set of images of 24 endometrial biopsies with NCSs and one without. Specifically, two independent observers counted an average of 15,473 nuclei and 928 NCSs. To assess intra-sample variation, 15 consecutive 7μm-thick paraffin sections were prepared and 5 randomly selected sections (#1, 6, 9, 12, and 14) analyzed for % EECs with NCSs. A total of 3,959 nuclei and 907 NCSs were counted.

To assess the local distribution of NCSs throughout the different layers of the endometrium, paraffin sections from all six regions of a single uterus were H&E stained and the images of the individual regions stitched together using Adobe Photoshop CS5 (Adobe Systems Inc., Mountain View, CA). The imaged epithelium was evenly divided into three layers (basal, middle, and luminal) and the number of glands for each layer determined. The number of NCSs in each layer was counted in immunostained paraffin sections that were successive to the H&E stained sections.

Outcome Measures and Statistical Analyses

To evaluate interobserver variability, we calculated the intraclass correlation coefficient (ICC) for the number of EECs and NCSs counted by two independent observers in 25 luteal endometrial biopsies using Stata 11.0 (Stata Corporation, College Station, TX). Additionally the correlation coefficient for the percent EECs with NCSs obtained between the two observers was calculated.

We tested our hypothesis that NCSs manifest a differential appearance pattern by uterine region. Our outcome of interest was the average % EECs with NCSs for each uterine region. To determine the distribution of our data, a Shapiro-Wilk normality test was performed with Prism 5 (GraphPad Software Inc., La Jolla, CA). Due to the lack of normal distribution in two regions, a one-way ANOVA (Friedman Test) for nonparametric paired data was applied ($p = 0.0008$) followed by a Wilcoxon signed ranks test for post-hoc analysis. Friedman and Wilcoxon tests were performed using R: A Language and Environment for Statistical Computing (R Foundation for Statistical Computing, Vienna, Austria).

RESULTS

A quantitative method for NCS assessment was developed returning % EECs with NCSs per endometrial biopsy (Fig 1A). Agreement between two independent observers on 25 samples for % EECs with NCSs was excellent ($r^2 = 0.99$; linear regression), as well as for the total count of NCSs (ICC = 0.96; 95% confidence interval [CI]: 0.93 to 1.00) and EECs (ICC = 0.97; 95% CI: 0.96 to 0.98). The high degree of agreement justifies the use of a single observer with our new NCS quantification method. Additionally, based on the % EECs with NCSs of 5 different paraffin sections from the same sample (22.8% +/−1.3%), the intra-sample variability of the assay was low (CV = 0.06).

Overall, 42 hysterectomy specimens were enrolled, 30 of which were declared as secretory-phase endometria by the clinical pathologist. Classic histologic dating was successfully performed on 29 of the 30 secretory-phase specimens; one specimen had insufficient tissue for definitive dating. Ten uteri were given histologic dates between CD 18-24. Of these, 9 had sufficient tissue for further analysis and 8 exhibited over 5% EECs with NCSs in at least

one of the six sampled regions of the endometrial cavity, as did the lone undated specimen, for a total of 9 uteri (Table 2).

NCSs appeared uniformly in the upper uterine cavity among these 9 uteri (Fig. 1B). Collectively, the upper 5 regions (excluding the LUS) demonstrated a median number of EECs with NCSs of 16.9% (IQR = 12.7-23.4), whereas the number of EECs with NCSs in the LUS of 6.1% (IQR = 3.0-9.9) was significantly lower ($p = 0.008$, Wilcoxon signed ranks test; Fig. 1B). Analysis of the endometrial layers in all six regions of one uterus (Fig. 1B, yellow dots; Table 2, #9), demonstrated that NCSs were predominant in the stratum functionalis, the luminal (38% +/−9%) and middle layers (46% +/−9%), as compared to the basal layer (17% +/−6%; $p = 0.004$, oneway ANOVA; Fig. 1C). In contrast, the number of glands was evenly distributed between the three layers (luminal: 27% +/−9%, middle: 36% +/−4%, basal: 37% +/−8%; $p = 0.132$; Fig. 1C).

DISCUSSION

We demonstrate that one of the histologic hallmarks of secretory transformation and a marker for the midluteal endometrium, the NCS, is equally present in fundal, cornual (left and right), and mid-cavity (anterior and posterior) uterine sections. Clearly, there is no predisposition for the cornua. These findings are consistent with a morphometric study wherein 11 of 12 indices among endometrial biopsies taken from three different regions failed to show differences (25); and which forms the basis for the use of a single, presumably fundal, endometrial biopsy specimen in clinical practice. Regardless, our results are surprising given the specificity of the NCS for the midluteal phase (6,7) and the decades of ultrastructural data setting the NCS apart from other histologic criteria and suggesting a role for it in endometrial receptivity (see Introduction). Overall, our data reinforce that secretory transformation is not region-specific, lags only in the LUS, and suggest that, similarly, endometrial receptivity is achieved in a uniform fashion.

Human embryo implantation is subject to strict temporal specificity, known as the implantation window, which is limited to CD 20-24 based on results from anatomic dissection (20), an ovum donor/recipient model (26), and epidemiologic surveillance using urinary hormonal metabolites (27). The question as to whether there is spatial specificity, or predisposition for implantation in (a) particular region(s) of the endometrial cavity, had been addressed by only a few studies (Table 1), and remains unresolved. In fact, despite the remarkable changes the endometrium undergoes each month, there is little information about local fluctuations. Additionally, a literature does exist regarding the optimal placement of the catheter tip during the embryo transfers (28-31). Those studies, however, merely establish the importance of avoiding fundal contact and the deleterious uterine contractility that ensues and, perhaps, the utility of an embryo transfer directed toward the lower or middle portions of the endometrial cavity, rather than toward the fundus. They are not definitive regarding the specific location frequencies of implantation. On the other hand, the studies in Table 1 collectively suggest that the cornual region might prove most favorable for blastocyst implantation. Indeed, a reported criterion for ultrasonographically differentiating a gestational sac from a pseudogestational sac is the eccentric (lateral) location of the former, versus the central (midline) presentation of the latter (32). Anatomic

rationale attributes the lateral predisposition of blastocyst implantation to the superior vascularization of the lateral endometrium and cornua due to abundant anastomoses of the ascending uterine and adnexal vasculature (32,33). Also, the free floating blastocyst might prefer the ipsilateral cornu either due to having encountered it first upon its egress from the fallopian tube or due to heretofore uncharacterized localized signaling.

Regardless, NCS prevalence is uniform in the upper endometrial cavity, and undisturbed by such lateral predisposition. The significantly lower prevalence of the NCS in the LUS is consistent with previous studies. Noyes et al. (21) already noted the lag in secretory transformation of the lower uterine segment – “Tissue from the fundus of the uterus gives more reliable information than that from the lower uterine segment,” and this finding has been endorsed in the subsequent literature (34). This defect in secretory transformation seems at least partially responsible for the low likelihood of lower segment implantation in unscarred uteri (placenta previa).

In addition to a preference for the upper endometrial cavity, NCSs show a preference for the endometrial luminal and middle layers in all uterine regions as compared to the basal layer (Fig. 1C). This is in contrast to the even distribution of glands. NCS prevalence in the luminal and middle layers highlights a hitherto unappreciated polarity of the endometrium and further underlines the physiological significance of NCSs, as those are the functionally important layers supporting implantation and being renewed during each cycle.

Of interest, the mere presence of intramural fibroids does not affect NCS appearance and, by extension, does not impede secretory transformation. The presence of intramural fibroids among our study specimens was ubiquitous (38/42, or 90% overall and 10/10, 100%, among the midluteal specimens), and is not surprising given that we specifically targeted benign hysterectomy specimens among ovulatory women under age 50. The fact that the 9 specimens with >5% EECs with NCSs in at least one region demonstrate >5% EECs with NCSs in every region that was sampled (Fig. 1 and Table 2), gives us confidence that intramural fibroids do not impede secretory transformation, and that this assertion is not vulnerable to type II error.

In summary, we used the region-specific appearance pattern of NCSs in the endometrial cavity to elucidate the question of regional predisposition for secretory transformation. Our finding that NCS presence is uniform throughout the upper endometrial cavity suggests symmetric transformation of the secretory-phase endometrium in the upper cavity – a process that appears impervious to the mere presence of intramural fibroids.

Acknowledgments

We thank Nanette Santoro (University of Colorado, Denver, CO) for her support of our work and for critical comments on the manuscript. We acknowledge the assistance of the Gynecology Service attending physicians and house staff at Montefiore Medical Center in enrolling hysterectomy specimens for this study. We are grateful to the Surgical Pathology staff at Montefiore Medical Center, Weiler Division (Charles Fernandez, Duhane McGregor, and Lin Zhang) for their assistance in obtaining the endometrial tissue sections. Statistical support was provided by the Einstein-Montefiore Institute for Clinical and Translational Research. All imaging was performed at the Analytical Imaging Facility and all slides were prepared by the Histotechnology and Comparative Pathology Facility of the Albert Einstein College of Medicine.

Financial Support: March of Dimes Birth Defects Foundation (#1-FY09-363 to UTM); CMBG Training Program (T32 GM007491 to MJS)

REFERENCES

1. Cornillie FJ, Lauweryns JM, Brosens IA. Normal human endometrium. An ultrastructural survey. Gynecol Obstet Invest. 1985; 20:113–29. [PubMed: 4085915]
2. Dubrauszky V, Pohlmann G. Strukturveränderungen am Nukleolus von Korpusendometriumzellen während der Sekretionsphase. Naturwissenschaften. 1960; 47:523–4.
3. Terzakis JA. The nucleolar channel system of human endometrium. J Cell Biol. 1965; 27:293–304. [PubMed: 5884628]
4. Spornitz UM. The functional morphology of the human endometrium and decidua. Adv Anat Embryol Cell Biol. 1992; 124:1–99. [PubMed: 1561944]
5. Clyman MJ. A new structure observed in the nucleolus of the human endometrial epithelial cell. Am J Obstet Gynecol. 1963; 86:430–2. [PubMed: 14021802]
6. Guffanti E, Kittur N, Brodt ZN, Polotsky AJ, Kuokkanen SM, Heller DS, et al. Nuclear pore complex proteins mark the implantation window in human endometrium. J Cell Sci. 2008; 121:2037–45. [PubMed: 18505792]
7. Rybak EA, Szmyga MJ, Zapantis G, Rausch M, Beshay VE, Polotsky AJ, et al. The nucleolar channel system reliably marks the midluteal endometrium regardless of fertility status: a fresh look at an old organelle. Fertil Steril. 2011; 95:1385–1389.e1. [PubMed: 21067716]
8. Dockery P, Pritchard K, Taylor A, Li TC, Warren MA, Cooke ID. The fine structure of the human endometrial glandular epithelium in cases of unexplained infertility: a morphometric study. Hum Reprod. 1993; 8:667–73. [PubMed: 8314956]
9. Dockery P, Pritchard K, Warren MA, Li TC, Cooke ID. Changes in nuclear morphology in the human endometrial glandular epithelium in women with unexplained infertility. Hum Reprod. 1996; 11:2251–6. [PubMed: 8943538]
10. Pryse-Davies J, Ryder TA, MacKenzie ML. In vivo production of the nucleolar channel system in post menopausal endometrium. Cell Tissue Res. 1979; 203:493–8. [PubMed: 519737]
11. Demir R, Kayisli UA, Celik-Ozenci C, Korgun ET, Demir-Weusten AY, Arici A. Structural differentiation of human uterine luminal and glandular epithelium during early pregnancy: an ultrastructural and immunohistochemical study. Placenta. 2002; 23:672–84. [PubMed: 12361686]
12. Kohorn EI, Rice SI, Gordon MM. In vitro production of nucleolar channel system by progesterone in human endometrium. Nature. 1970; 228:671–2. [PubMed: 5474940]
13. Kohorn EI, Rice SI, Hemperly SS, Gordon MM. The relation of the structure of progestational steroids to nucleolar differentiation in human endometrium. J Clin Endocrinol. 1972; 34:257–64. [PubMed: 12256658]
14. Roberts DK, Horbelt DV, Powell LC. The ultrastructural response of human endometrium to medroxyprogesterone acetate. Am J Obstet Gynecol. 1975; 123:811–8. [PubMed: 173189]
15. Dockery P, Ismail RM, Li TC, Warren MA, Cooke ID. The effect of a single dose of mifepristone (RU486) on the fine structure of the human endometrium during the early luteal phase. Hum Reprod. 1997; 12:1778–84. [PubMed: 9308811]
16. More IA, McSeveney D. The three dimensional structure of the nucleolar channel system in the endometrial glandular cell: serial sectioning and high voltage electron microscopic studies. J Anat. 1980; 130:673–82. [PubMed: 7000735]
17. Cavagna M, Contart P, Petersen CG, Mauri AL, Martins AMC, Baruffi RLR, et al. Implantation sites after embryo transfer into the central area of the uterine cavity. Reprod Biomed Online. 2006; 13:541–6. [PubMed: 17007675]
18. Kawakami Y, Andoh K, Mizunuma H, Yamada K, Itoh M, Ibuki Y. Assessment of the implantation site by transvaginal ultrasonography. Fertil Steril. 1993; 59:1003–6. [PubMed: 8486166]
19. Minami S, Ishihara K, Araki T. Determination of blastocyst implantation site in spontaneous pregnancies using three-dimensional transvaginal ultrasound. Journal of Nippon Medical School = Nihon Ika Daigaku zasshi. 2003; 70:250–4.

20. Hertig A, Rock J, Adams EC. A description of 34 human ova within the first 17 days of development. Am J Anat. 1956; 98:435–93. [PubMed: 13362122]
21. Noyes RW, Hertig A, Rock J. Dating the Endometrial Biopsy. Fertil Steril. 1950; 1:3–25.
22. Murray M, Meyer W, Zaino R, Lessey B, Novotny D, Ireland K, et al. A critical analysis of the accuracy, reproducibility, and clinical utility of histologic endometrial dating in fertile women. Fertil Steril. 2004; 81:1333–43. [PubMed: 15136099]
23. Werner M, Chott A, Fabiano A, Battifora H. Effect of formalin tissue fixation and processing on immunohistochemistry. Am J Surg Pathol. 2000; 24:1016–9. [PubMed: 10895825]
24. Houghton JP, Roddy SS, Carroll SS, McCluggage WG. A simple method for the prevention of endometrial autolysis in hysterectomy specimens. Journal of Clinical Pathology. 2004; 57:332–3. [PubMed: 14990613]
25. Johannisson EE, Parker RAR, Landgren BMB, Diczfalusy EE. Morphometric analysis of the human endometrium in relation to peripheral hormone levels. Fertil Steril. 1982; 38:564–71. [PubMed: 7128842]
26. Bergh PA, Navot D. The impact of embryonic development and endometrial maturity on the timing of implantation. Fertil Steril. 1992; 58:537–42. [PubMed: 1521649]
27. Wilcox AJ, Baird DD, Weinberg CR. Time of implantation of the conceptus and loss of pregnancy. N Engl J Med. 1999; 340:1796–9. [PubMed: 10362823]
28. Waterstone J, Curson R, Parsons J. Embryo transfer to low uterine cavity. Lancet. 1991; 337:1413–3. [PubMed: 1674783]
29. Coroleu B, Barri PN, Carreras O, Martínez F, Parriego M, Hereter L, et al. The influence of the depth of embryo replacement into the uterine cavity on implantation rates after IVF: a controlled, ultrasound-guided study. Hum Reprod. 2002; 17:341–6. [PubMed: 11821275]
30. Frankfurter D, Trimarchi JB, Silva CP, Keefe DL. Middle to lower uterine segment embryo transfer improves implantation and pregnancy rates compared with fundal embryo transfer. Fertil Steril. 2004; 81:1273–7. [PubMed: 15136089]
31. Pope CS, Cook EKD, Arny M, Novak A, Grow DR. Influence of embryo transfer depth on in vitro fertilization and embryo transfer outcomes. Fertil Steril. 2004; 81:51–8. [PubMed: 14711544]
32. Abramovici H, Auslender R, Lewin A, Faktor JH. Gestational-pseudogestational sac: a new ultrasonic criterion for differential diagnosis. Am J Obstet Gynecol. 1983; 145:377–9. [PubMed: 6824027]
33. Itskovitz J, Lindenbaum ES, Brandes JM. Arterial anastomosis in the pregnant human uterus. Obstet Gynecol. 1980; 55:67–71. [PubMed: 7352063]
34. Robertson W. A reappraisal of the endometrium in infertility. Clin Obstet Gynaecol. 1984; 11:209–26. [PubMed: 6370533]

CAPSULE

Nucleolar channel systems appear uniformly throughout the upper endometrial cavity, excluding the lower uterine segment, and preferentially in the functional, luminal layers of the endometrium indicating uniform secretory transformation.

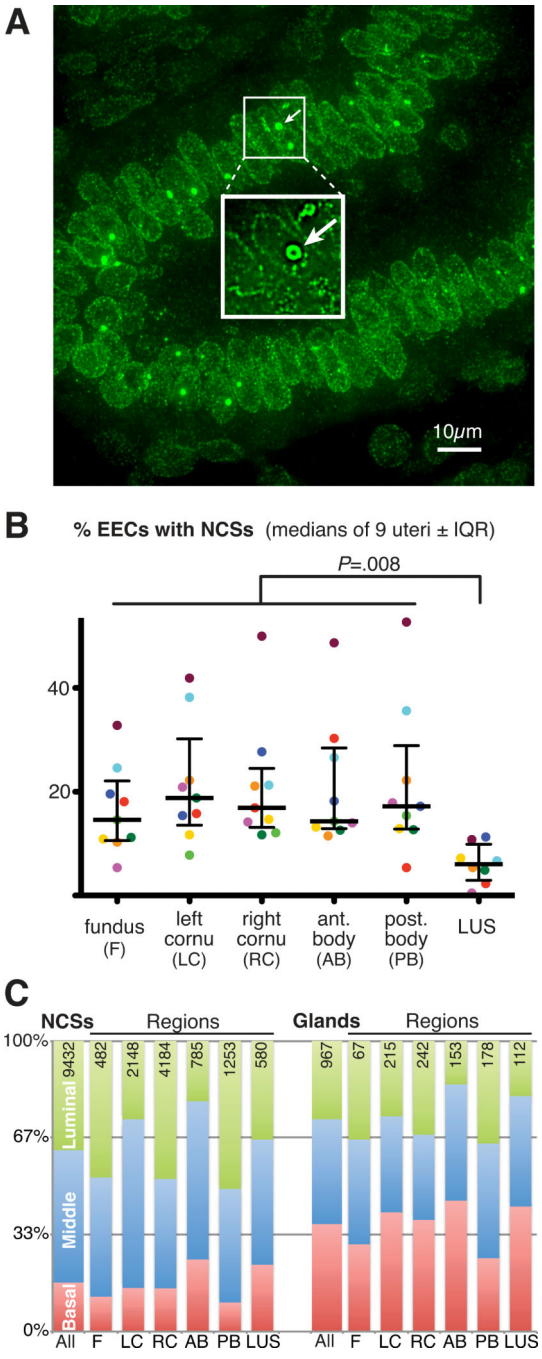

Figure 1.

(A) Endometrial gland: indirect immunofluorescence of nuclear pore complex proteins that are highly enriched in NCSs (one is highlighted by an arrow) on one of the ten random optical fields analyzed for the anterior body region of one uterus (red in B). A maximum projection of 22 0.3μm-thick optical sections is shown. Inset: twofold magnification of a single optical section from the boxed area above; note, in that optical plane only two of the three NCSs seen in the maximum projection are visible (i.e., the NCS in the lower right

corner is situated on a different plane), and note the outline of the nuclear boundary by the individual pore complexes.

(B) Regional prevalence of NCSs in the uterus. % EECs with NCSs in six regions of 9 uteri (colors correspond to the following numbers in Table 2: blue = 1, light green = 2, purple =3, light blue = 4, orange = 5, red = 6, brown = 7, green = 8, yellow = 9). The medians ± interquartile range (IQR) are indicated for each region, as is the significant difference between the lower uterine segment and the other five regions ($p = 0.008$, Wilcoxon signed ranks test).

(C) Prevalence of NCSs in the endometrial layers. The distribution of NCSs (left) and Glands (right) between three equal layers (basal, middle, and luminal) of the endometrium of one uterus (yellow in B) is indicated for all regions together (first column each) and for each individual region (abbreviations as in B). The numbers correspond to 100% of each column. Note the reduced amount of NCSs in the basal layer compared to the middle and luminal ones.

TABLE 1

Studies investigating the region-specific implantation frequency of blastocysts within the endometrial cavity

Study	Hertig 1956	Kawakami 1993	Minami 2003	Cavagna 2006
Design	Anatomic dissection of 211 hysterectomy specimens derived from women of known fertility; a subset of which were derived from women during the luteal phase with early pregnancies, some having already implanted	2-Dimensional Transvaginal Ultrasonography on fertility clinic patients during the follicular phase and prior to 6 weeks gestation dated by basal body temperature	3-Dimensional Transvaginal Ultrasonography on unselected women with gestational sacs measuring 3-6mm	3-Dimensional Transvaginal Ultrasonography performed 21-24 days after embryo transfer (ET) on women with singleton pregnancies having undergone ICSI and ultrasound-guided ET intentionally directed to the midpoint between the internal os and fundus
Sample size Conception	26 spontaneous	21 spontaneous	138 spontaneous	47 assisted
Fundus (midline)	**100% in upper cavity:** 58% ipsilateral to corpus luteum 4% midline 38% contralateral to corpus luteum	**Upper versus middle cavity not specified:** 81% ipsilateral to dominant follicle 14% midline 5% contralateral to dominant follicle	16%	34%
Left Cornu			39%	15%
Right Cornu			34%	17%
Anterior Body			9% middle cavity region	30% middle cavity region
Posterior Body				
Lower uterine Segment			2%	4%

TABLE 2

Patient information and NCS prevalence by uterine region

Patient	**1**	**2**	**3**	**4**	**5**	**6**	**7**	**8**	**9**	**Average ± SD**
Age	42	41	47	42	42	45	43	44	46	43.6 ± 2.1
Cycle Day (LMP)	20	22	NA	19	17	23	24	19	19	20.4 ± 2.4
Cycle Day (Noyes)	20	23	NA	18	18	19	19	20	19	19.5 ± 1.6
Parous	+	-	+	+	+	+	+	+	+	8/9
Intramural Fibroids	+	+	+	+	+	+	+	+	+	9/9
Submucosal Fibroids	+	+	+	-	-	-	-	-	+	4/9
% EECs with NCSs										**Median (IQR)**
Fundus(F)	19.6	14.6	5.4	24.6	10.3	18.1	32.8	11.2	10.9	14.6 (10.6-22.1)
Left Cornu (LC)	15.4	7.8	20.9	38.2	22.2	15.8	41.9	18.8	11.7	18.8 (13.6-30.2)
Right Cornu (RC)	27.7	12.1	14.2	21.3	21.1	16.9	50.0	11.7	14.7	16.9 (13.2-24.5)
Anterior Body (AB)	18.2	14.3	14.0	26.6	11.5	30.3	48.7	12.6	13.2	14.3 (12.9-28.5)
Posterior Body (PB)	17.2	15.4	17.9	35.6	22.2	5.4	52.7	12.7	12.9	17.2 (12.8-28.9)
Lower Uterine Segment (LUS)	11.3	NA	0.5	6.7	5.4	2.3	10.8	4.9	7.2	6.1 (3.0-9.9)